JCI insight

RESEARCH ARTICLE

IP_3 receptors regulate vascular smooth muscle contractility and hypertension

Qingsong Lin,[1] Guiling Zhao,[2] Xi Fang,[3] Xiaohong Peng,[1] Huayuan Tang,[1] Hong Wang,[1] Ran Jing,[4] Jie Liu,[5] W. Jonathan Lederer,[2] Ju Chen,[3] and Kunfu Ouyang[1]

[1]Drug Discovery Center, Key Laboratory of Chemical Genomics, Peking University Shenzhen Graduate School, Shenzhen, China. [2]Center for Biomedical Engineering and Technology, University of Maryland School of Medicine, Baltimore, Maryland, USA. [3]University of California San Diego, School of Medicine, Department of Medicine, La Jolla, California, USA. [4]Xiangya Hospital, Central South University, Changsha, China. [5]Department of Pathophysiology, School of Medicine, Shenzhen University, Shenzhen, China.

Inositol 1, 4, 5-trisphosphate receptor–mediated (IP_3R-mediated) calcium (Ca^{2+}) release has been proposed to play an important role in regulating vascular smooth muscle cell (VSMC) contraction for decades. However, whether and how IP_3R regulates blood pressure in vivo remains unclear. To address these questions, we have generated a smooth muscle–specific IP_3R triple-knockout (smTKO) mouse model using a tamoxifen-inducible system. In this study, the role of IP_3R-mediated Ca^{2+} release in adult VSMCs on aortic vascular contractility and blood pressure was assessed following tamoxifen induction. We demonstrated that deletion of IP_3Rs significantly reduced aortic contractile responses to vasoconstrictors, including phenylephrine, U46619, serotonin, and endothelin 1. Deletion of IP_3Rs also dramatically reduced the phosphorylation of MLC20 and MYPT1 induced by U46619. Furthermore, although the basal blood pressure of smTKO mice remained similar to that of wild-type controls, the increase in systolic blood pressure upon chronic infusion of angiotensin II was significantly attenuated in smTKO mice. Taken together, our results demonstrate an important role for IP_3R-mediated Ca^{2+} release in VSMCs in regulating vascular contractility and hypertension.

Introduction

Numerous studies have validated the essential role of calcium (Ca^{2+}) signaling in regulating blood pressure. For example, the blocking of voltage-operated Ca^{2+} channels (VOCCs) located in the plasma membrane, which mediate Ca^{2+} influx and increase intracellular Ca^{2+} levels, significantly reduces high blood pressure in hypertensive patients (1–3). However, the role of intracellular Ca^{2+} release channels, such as ryanodine receptors and inositol 1, 4, 5-trisphosphate receptors (IP_3Rs), localized in the membrane of endoplasmic reticulum (ER), has yet to be fully elucidated in blood pressure homeostasis.

The IP_3R has 3 different subtypes (IP_3R1, IP_3R2, and IP_3R3) in mammals, which are encoded by 3 genes, *Itpr1*, *Itpr2*, and *Itpr3*, respectively. IP_3R subtypes are expressed in diverse tissues to varying degrees (4), yet all are expressed in vascular smooth muscle cells (VCMCs) (5–7). As one of the major sources of intracellular Ca^{2+} release, IP_3Rs have been implicated in regulating many biological processes. Deficiency of distinct subtypes of IP_3Rs in mice has been shown to cause severe abnormalities and diseases, including ataxia and epileptic seizures (8), exocrine secretion defects (9–11), abnormal taste perception (12), embryonic developmental defects (13, 14), and T cell acute lymphoblastic leukemia (15).

In vascular smooth muscles, IP_3R-mediated Ca^{2+} release has long been proposed to be a critical player in cellular contraction, and the underlying signaling pathways are well established. In brief, upon binding of a vasoconstrictive agonist to the membrane GPCRs (primarily Gq/11-coupled subtypes), phospholipase Cβ (PLCβ) is activated and thus catalyzes phosphatidylinositol 4, 5-bisphosphate into diacylglycerol and 1, 4, 5-inositol trisphosphate (IP_3). The latter binds to IP_3Rs and causes Ca^{2+} channels to open, which subsequently leads to Ca^{2+} release from the ER and an increase in cytosolic Ca^{2+} concentration, thereby resulting in cell contraction (16, 17). To date, most studies describing IP_3R regulation of vascular smooth muscle contractility involve the use of IP_3R blockers (18–20).

Conflict of interest: The authors have declared that no conflict of interest exists.

Submitted: July 6, 2016
Accepted: September 20, 2016
Published: October 20, 2016

Reference information:
JCI Insight. 2016;1(17):e89402.
doi:10.1172/jci.insight.89402.

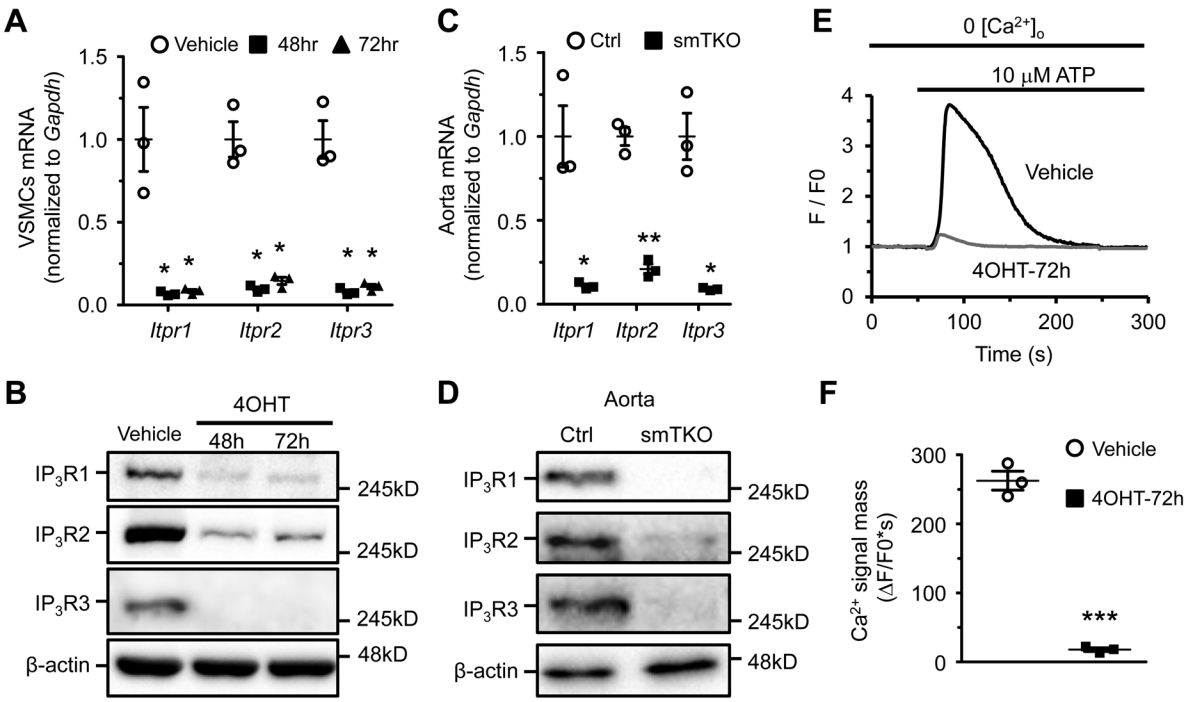

Figure 1. Characterization of IP_3R deletion in mouse vascular smooth muscle cells in vitro and in vivo. (**A** and **B**) Vascular smooth muscle cells (VSMCs) isolated from noninduced smTKO mice were cultured and treated with 1 μM 4-hydroxytamoxifen (4OHT) for 48 and 72 hours to induce IP_3R gene deletion. VSMCs treated with vehicle were used as the control (Ctrl). Administration of 4OHT significantly decreased the mRNA (**A**) and protein (**B**) levels of each IP_3R subtype compared with the vehicle treatment. $n = 3$ independent cultures per group. (**C** and **D**) mRNA (**C**) and protein (**D**) levels of each IP_3R subtype in aortas were assessed from control and smTKO mice. $n = 3$ (with vessels from 3 mice pooled as one sample) per group. (**E**) Representative curves of Ca^{2+} release induced by 10 μM ATP in cultured VSMCs treated with vehicle (black) or 4OHT for 72 hours (gray). Cells were incubated with 5 μM fluo-4-AM at 37°C for 30 minutes and imaged with confocal microscopy. Cells were perfused in Ca^{2+}-free solution for 1 to 2 minutes to eliminate Ca^{2+} entry via membrane ionotropic purinergic receptors prior to the administration of ATP. (**F**) Averaged Ca^{2+} signal mass calculated from the time course of Ca^{2+} release induced by ATP in VSMCs. $n = 3$ independent tests per group, and at least 20 cells per experiment were imaged. Significance was determined by the 2-tailed, unpaired Student's t test. $^*P < 0.05$, $^{**}P < 0.01$, $^{***}P < 0.001$.Data represent mean ± SEM.

Although all 3 single global IP_3R knockout mice and all 3 double-combination IP_3R knockout mice have been previously generated, these mice are not suitable to investigate the role of IP_3Rs in VSMCs in vivo because most develop severe phenotypes that could potentially affect cardiovascular development and physiology (8–10, 13, 14). In addition, different IP_3R subtypes could function redundantly in regulating vascular contractility and blood pressure, since it has been shown that all 3 subtypes are expressed in VSMCs (20–22).

To overcome the aforementioned issues, we generated a smooth muscle–specific IP_3R triple-knockout (smTKO) mouse model using a tamoxifen-inducible system, which allowed us to delete all 3 IP_3Rs in adult mouse smooth muscle cells. Using this mouse model, we investigated the function of IP_3Rs in regulating vascular contractility and blood pressure in vivo.

Results

Expression and deletion of IP_3Rs in VSMCs. Since IP_3R1 has been proposed to be the predominant subtype in VSMCs (22, 23), we initially created a smooth muscle–specific IP_3R1 knockout mouse using Sm22α-Cre (Supplemental Figure 1A; supplemental material available online with this article; doi:10.1172/jci.insight.89402DS1). We found that deletion of IP_3R1 in VSMCs (R1-KO) significantly reduced, but was not able to abolish, ATP-induced intracellular Ca^{2+} release (Supplemental Figure 1, B and C): the Ca^{2+} signal mass induced by ATP in R1-KO cells was only decreased by 48% compared with control cells (144.1 ± 15.2 ΔF/F0·s in control cells vs. 275.3 ± 10.4 ΔF/F0·s in R1-KO cells). Furthermore, the expression of IP_3R3 in the aorta was increased when IP_3R1 was conditionally deleted (Supplemental Figure 1A). Taken together, these results strongly suggested that the other two IP_3R subtypes might play a compensatory role in VSMCs when IP_3R1 was deleted.

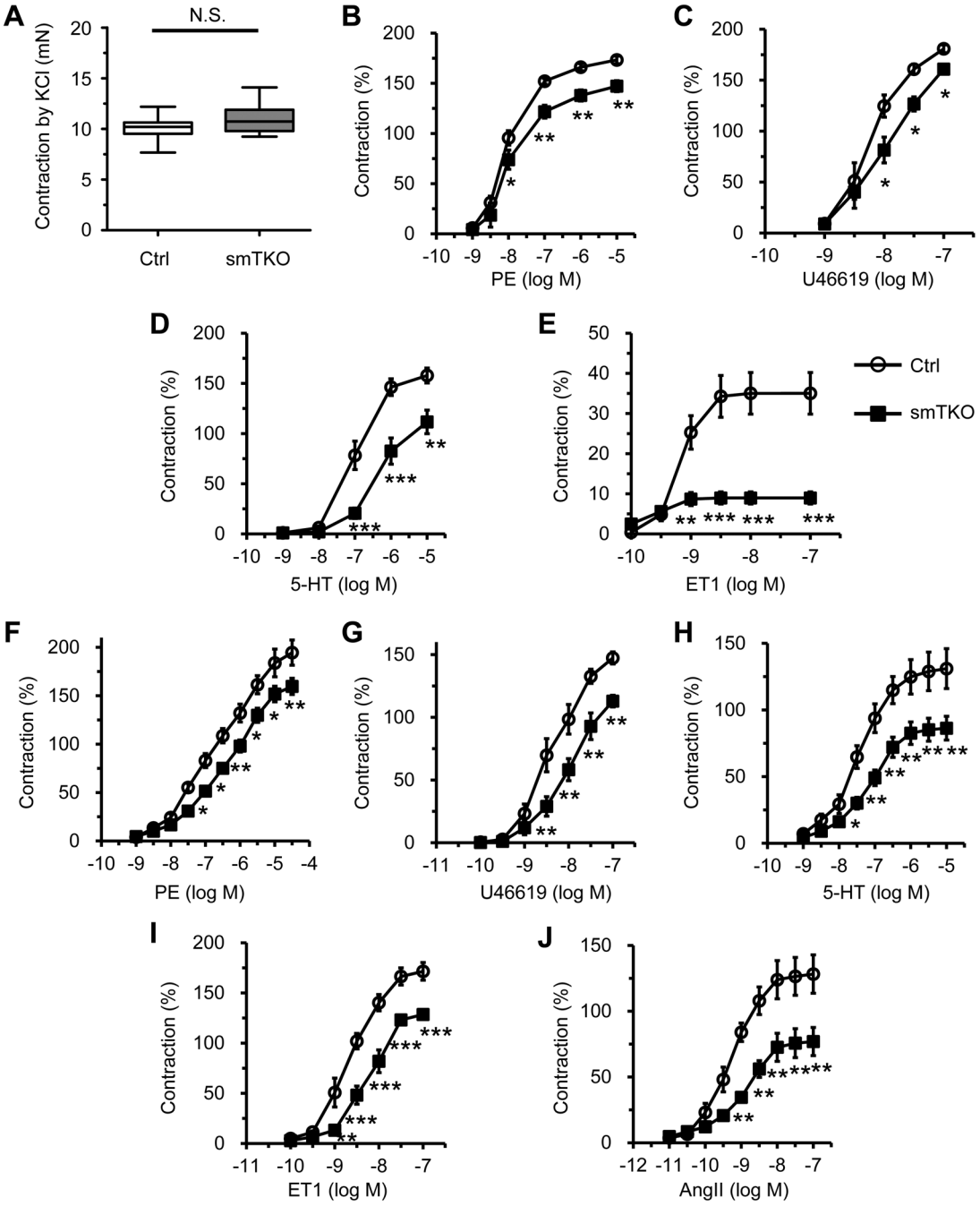

Figure 2. Loss of IP_3Rs reduced vascular contractile responses to various vasoconstrictors. Thoracic aortas and the first-order branch of superior mesenteric arteries were isolated from control (Ctrl) and smTKO mice. The vessels were cut into 2-mm-long segments, and myographic measurements were performed. (**A**) Reference contraction of aortic rings induced by high potassium (100 mM) in control and smTKO mice. *n* = 6–11 mice per group. Significance was determined by the 2-tailed, unpaired Student's *t* test. In the box-and-whisker plot, the center lines indicate the mean and the upper and lower bounds of the boxes represent the 25th–75th percentiles of the averaged data. (**B–E**) Tension induced by phenylephrine (PE), U46619, 5-hydroxytryptamine (5-HT), and endothelin 1 (ET1) in control and smTKO aortic rings. (**F–J**) Tension induced by PE, U46619, 5-HT, ET1, and angiotensin II (AngII) in control and smTKO mesenteric arteries. *n* = 6 mice per group. For all dose-response curves, data were expressed as a percentage of the peak of K^+-induced contraction, and significance was determined by 2-way ANOVA analysis with Bonferroni post-hoc test. $^*P < 0.05$, $^{**}P < 0.01$, $^{***}P < 0.001$ vs. control. Data represent mean ± SEM.

To further understand the physiological function of IP_3R-mediated Ca^{2+} release in the regulation of vascular contractility and blood pressure in vivo, we generated a smTKO mouse. Initially, we crossed Sm22α-Cre, as above, with IP_3R triple flox ($IP_3R1^{f/f}IP_3R2^{f/f}IP_3R3^{f/f}$) (f/f) mice. However, deletion of all IP_3R subtypes by Sm22α-Cre resulted in leukemia and premature lethality (Supplemental Figure 2), which was similar to what we observed in $IP_3R1^{f/f}IP_3R2^{f/f}IP_3R3^{f/f}$/Tie2-$Cre^+$ mice (15). This is consistent with a

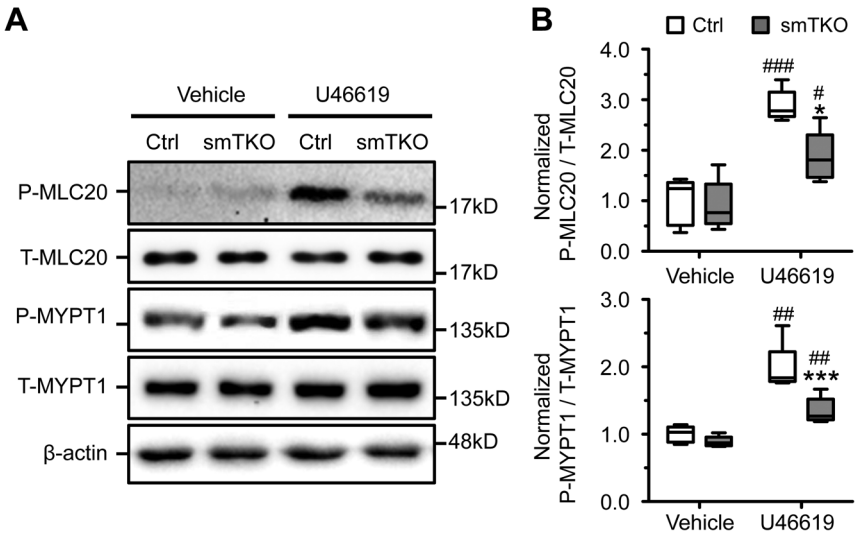

Figure 3. IP_3R deficiency repressed U46619-induced myosin light chain 20 and myosin-binding regulatory subunit phosphorylation. Protein was isolated from control (Ctrl) and smTKO thoracic aortas treated with either vehicle or U46619 (0.1 μM). (**A**) The phosphorylation of myosin light chain 20 (MLC20) and myosin-binding regulatory subunit (MYPT1) was measured by Western blot. (**B**) The levels of phosphorylated MLC20 and MYPT1 were normalized to total MLC20 and MYPT1, respectively, and averaged. $n = 5$ (with vessels from 2 mice pooled as one sample) per group. Significance was determined by 2-way ANOVA analysis with Bonferroni post-hoc test. $^*P < 0.05$, $^{***}P < 0.001$ vs. control. $^{\#}P < 0.05$, $^{\#\#}P < 0.01$, $^{\#\#\#}P < 0.001$ vs. vehicle. In box-and-whisker plots, center lines indicate the mean and the upper and lower bounds of the boxes represent the 25th–75th percentiles of the averaged data.

previous study showing that Sm22α-Cre is also expressed in myeloid cell lineages (24). We then bred IP_3R triple flox mice with SMMHC-CreER^{T2} mice, which express a fusion protein of Cre recombinase with a modified estrogen receptor–binding domain under the control of the smooth muscle–specific smooth muscle myosin heavy chain (SMMHC) promoter (25). Male $IP_3R1^{f/f}IP_3R2^{f/f}IP_3R3^{f/f}$/SMMHC-Cre$^+$ mice aged 7 to 8 weeks were then intraperitoneally injected with tamoxifen (50 mg/kg, 5 consecutive days) and considered as smTKO mice. We first examined if SMMHC-Cre could efficiently delete IP_3R genes upon administration of tamoxifen. In cultured VSMCs that were isolated from noninduced smTKO aortas, addition of 4-hydroxytamoxifen (4OHT) into the medium could efficiently abolish the mRNA and protein levels of all 3 IP_3R subtypes at both 48 hours and 72 hours after treatment (Figure 1, A and B). At 1 month after tamoxifen injection, the expression of all 3 IP_3R subtypes in the aortas isolated from smTKO mice was also significantly reduced compared with control mice (Figure 1, C and D). Interestingly, deletion of all 3 IP_3R subtypes resulted in a more dramatic decrease in ATP-induced intracellular Ca^{2+} release, compared with single IP_3R1 deletion. The Ca^{2+} signal mass induced by ATP in IP_3R triple-knockout VSMCs was decreased by 93% compared with control cells (17.9 ± 5.3 ΔF/F0·s in IP_3R triple-knockout cells vs. 262.5 ± 11.3 ΔF/F0·s in control cells; Figure 1, E and F). Taken together, these results demonstrated that IP_3R1 alone does not suffice to mediate ATP-induced intracellular mobilization in VSMCs, whereas IP_3R1 plus least one other isoform (IP_3R2 or IP_3R3 or both) does. We also investigated whether deletion of IP_3Rs affects intracellular Ca^{2+} signals induced by an agonist that does not activate an ionotropic receptor in VSMCs. Consistently, we found that the Ca^{2+} signal mass induced by 5-hydroxytryptamine (5-HT), U46619, and endothelin 1 (ET1) was reduced by 94.0%, 90.8%, and 90.4%, respectively, in IP_3R triple-knockout VSMCs when compared with control cells (Supplemental Figure 3). Furthermore, we examined whether deletion of IP_3Rs affects VSMC Ca^{2+} waves in intact vessels. We isolated posterior cerebral arteries from control and smTKO mice and measured spontaneous Ca^{2+} waves in smooth muscle cells. We found that the frequency of spontaneous Ca^{2+} waves in smTKO VSMCs is lower than in control cells. Moreover, application of ET1 (20 nM) significantly increased the frequency of spontaneous Ca^{2+} waves in control VSMCs, which was almost abolished in smTKO cells (Supplemental Figure 4).

Deletion of IP_3Rs attenuates vascular contractile response. To determine if deletion of IP_3Rs affects vascular contractility, we investigated the contractile function of arteries derived from control and smTKO mice using wire myography. Thoracic aortic rings were freshly prepared and pretreated with indomethacin and nitro-L-arginine to inhibit cyclooxygenases and endothelial nitric oxide synthase activity, respectively. We found that the potassium chloride–induced (KCl-induced) reference contraction did not significantly differ between control and smTKO mice (10.17 ± 0.23 mN in smTKO mice vs. 11.03 ± 0.30 mN in control mice; Figure 2A). However, although the vasoconstrictors, phenylephrine (PE), U46619, and 5-HT, were still able to induce contraction of smTKO vessels, their potency and efficacy were significantly decreased compared with control vessels (Figure 2, B–D). By contrast, ET1-induced vascular contraction was almost abolished

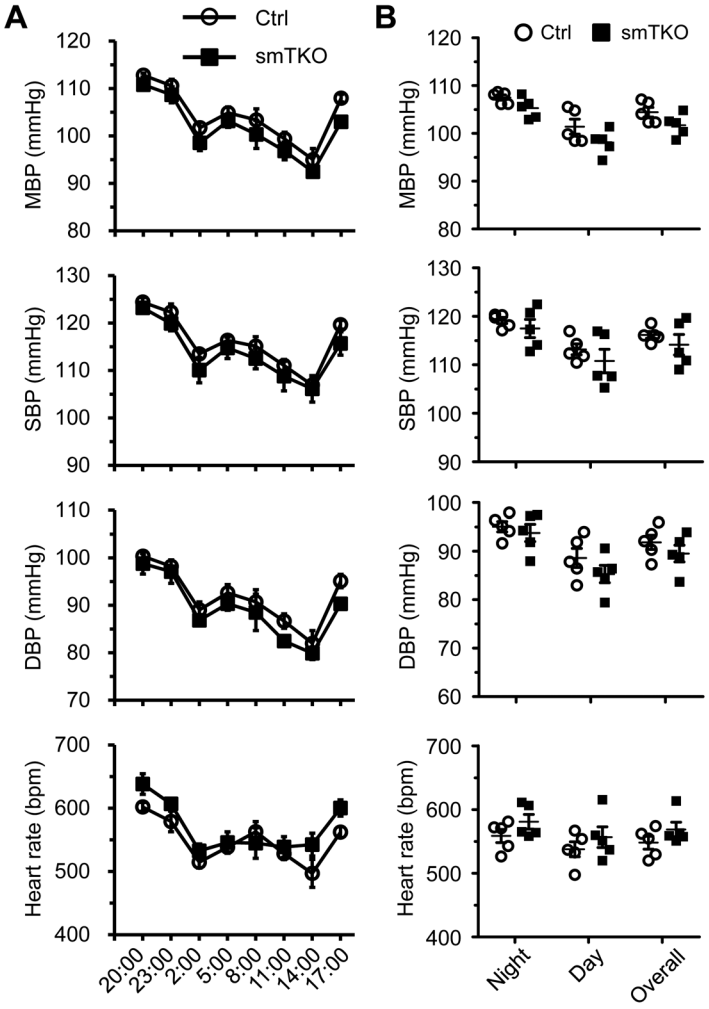

Figure 4. Normal basal blood pressure was observed in smTKO mice. Blood pressures and heart rate were measured in unrestrained mice using an implantable telemetry system. (**A**) Twenty-four hours of data are presented at times indicated on a 24-hour scale; data shown at each point represent 3-hour rolling averages of data sampled each minute. The data showed diurnal variations in mean blood pressure (MBP), mean systolic blood pressure (SBP), mean diastolic blood pressure (DBP), and heart rates in both control (Ctrl) and smTKO mice. smTKO mice showed comparable values at all time points compared to control mice. *n* = 5 mice per group. Significance was determined by 2-way ANOVA analysis with Bonferroni post-hoc test. Data represent mean ± SEM. (**B**) Mean values for MBP, SBP, DBP, and heart rates were calculated at peak night (20:00–2:00) and day (8:00–14:00) times. *n* = 5 mice per group. Significance was determined by 2-tailed, unpaired Student's *t* test. Data represent mean ± SEM.

in smTKO mice compared with control mice (Figure 2E). Furthermore, we examined contractile function in a resistance vessel, the mesenteric artery, which is more relevant to the control of blood pressure, as compared with the aortas studied above. Consistently, we found that the contraction of the mesenteric artery induced by PE, U46619, 5-HT, ET1, and angiotensin II (AngII) was significantly decreased in smTKO vessels compared with control vessels (Figure 2, F–J), while the reference contraction induced by KCl was not different between smTKO and control mice (4.14 ± 0.23 mN in smTKO mice vs. 3.51 ± 0.29 mN in control mice; $P = 0.10$ by 2-tailed, unpaired Student's *t* test). In addition, we found that pretreatment with 2-APB, an antagonist of IP_3R, did not cause further reduction in AngII-induced contraction in smTKO mesenteric arteries (Supplemental Figure 5).

We next examined the expression of major vasoconstrictive GPCRs in VSMCs, including adrenergic receptor α1a (*Adra1a*), α1b (*Adra1b*), and α1d (*Adra1d*); thromboxane A2 receptor (*Tbxa2r*); serotonin receptor 2A (*Htr2a*); angiotensin receptor type 1a (*Agtr1a*) and type 2 (*Agtr2*); and endothelin receptor type A (*Ednra*). The expression of these receptors was comparable between control and smTKO vessels, except for that of *Ednra*, which was decreased in smTKO vessels compared with control vessels (Supplemental Figure 6A). Furthermore, we investigated the expression of major Ca^{2+} channels expressed in VSMCs. Expression of other ER Ca^{2+} release channels, ryanodine receptor type 2 (*Ryr2*) and type 3 (*Ryr3*), voltage-gated L-type Ca^{2+} channel (*Cav1.2*), and stromal interaction molecule 1 (*Stim1*) and 2 (*Stim2*), did not significantly differ between control and smTKO vessels. Expression of PLCβ1 (*Plcb1*) was also not significantly changed in smTKO aortas compared with control aortas (Supplemental Figure 6B).

IP_3R deletion leads to repression of MLC20 and MYPT1 phosphorylation. The reduced sensitivity of vessels to contractile agonists in smTKO mice, in the absence of a reduction in GPCR expression, suggested altered expression or activity of contractile regulatory proteins. In VSMCs, phosphorylation of myosin light chain 20 (MLC20) is the primary regulatory event for the initiation of force production (26). MLC20 phosphorylation level is regulated by MLC kinase (MLCK) and phosphatase (MLCP), the latter consisting of a myosin-binding regulatory subunit (MYPT1), a catalytic subunit, and a 20-kDa subunit. Phosphorylation of MYPT1 decreases MLCP activity and therefore enhances MLC20 phosphorylation (27). Western blot analysis showed that expression of MLC20, MLCK, and MYPT1 in smTKO aortas is comparable to that of control aortas. Expression of Sm22α and α smooth muscle actin (SMA) was also not changed in smTKO aortas compared with control aortas (Supplemental Figure 7).

We then investigated if deletion of IP_3Rs affects the phosphorylation of MLC20 and MYPT1. Thoracic aortas were isolated from control and smTKO mice and incubated with PSS (vehicle) and U46619, respectively. In the vessels treated with vehicle, the phosphorylation levels of MLC20 at Ser19 and MYPT1

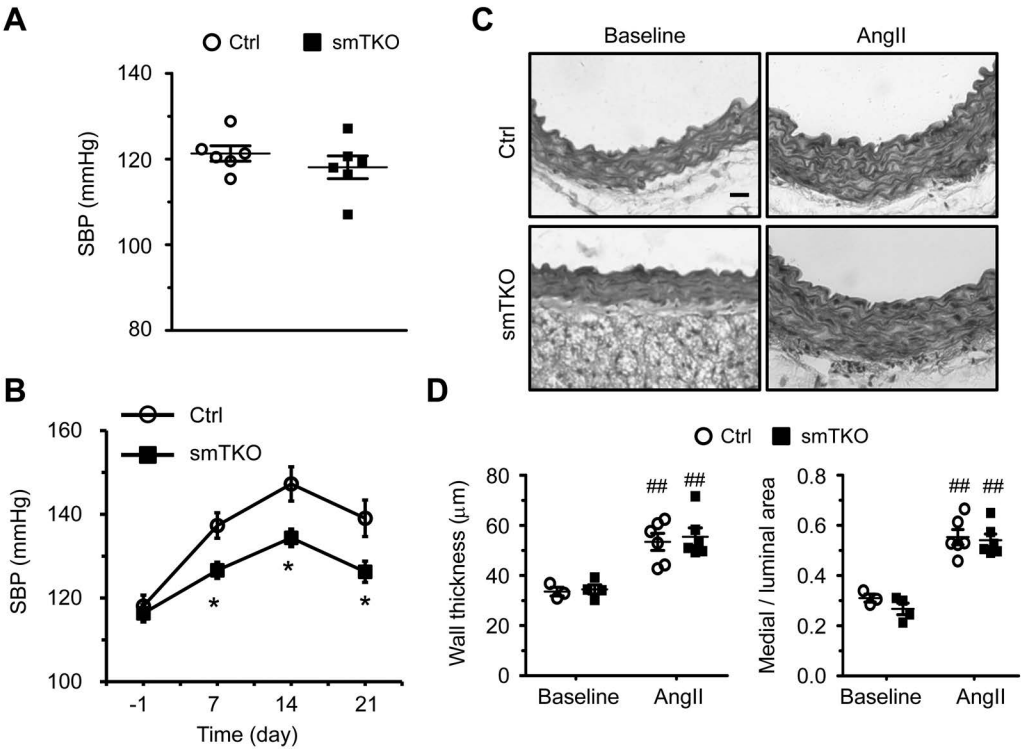

Figure 5. Deletion of IP_3Rs reduced angiotensin II–induced hypertension. Angiotensin II (AngII) was infused chronically for 21 consecutive days via a subcutaneously implanted osmotic mini-pump, and blood pressure was measured using the tail-cuff system. (**A**) Systolic blood pressure (SBP) measured in control (Ctrl) and smTKO mice prior to AngII infusion. n = 6 mice per group. Significance was determined by 2-tailed, unpaired Student's t test. (**B**) SBP measured at day –1, day 7, day 14, and day 21 after AngII infusion. n = 6 mice per group. Significance was determined by 2-way ANOVA analysis with Bonferroni post-hoc test. $^*P < 0.05$ vs. control. (**C**) Representative H&E-stained sections of control and smTKO thoracic aortas before (baseline) and after AngII infusion. Scale bar: 20 μm. (**D**) Vascular remodeling was accessed by measuring wall thickness and the ratio of medial to luminal area. n = 3–6 mice per group. Significance was determined by 2-way ANOVA analysis with Bonferroni post-hoc test. $^{\#\#}P < 0.01$ vs. baseline. Data represent mean ± SEM.

at Thr853 were relatively low, with no significant difference observed between control and smTKO mice (Figure 3). Administration of U46619, however, dramatically increased MLC20 and MYPT1 phosphorylation in both control and smTKO vessels (Figure 3), consistent with the increase in vessel contractility observed following administration of U46619 in vitro. Interestingly, deletion of IP_3Rs in VSMCs significantly attenuated the U46619-induced increase in phosphorylation of both MLC20 (increased by 1.88- ± 0.12-fold in control vs. 0.87- ± 0.20-fold in smTKO) and MYPT1 (increased by 0.97- ± 0.14-fold in control vs. 0.35 ± 0.08 fold in smTKO) (Figure 3).

Deletion of IP_3Rs does not affect basal blood pressure but diminishes AngII-induced hypertension. The impaired response to vasoconstrictive agonists observed in isolated vessels suggested that smTKO mice might exhibit evidence of diminished peripheral vascular resistance in vivo. To explore this possibility, in conscious and unrestrained mice, we used a telemetry system to analyze the hemodynamics of smTKO and control mice. The averaged results from data collected continuously over 24 hours showed that all the mice displayed characteristic diurnal variations in blood pressure and heart rate (Figure 4A). Furthermore, we did not observe any significant difference in mean blood pressure, mean systolic blood pressure, mean diastolic blood pressure, and mean heart rate between smTKO and control mice (Figure 4B), which together suggested that vascular smooth muscle IP_3Rs have no major contribution in maintaining basal blood pressure.

We further investigated if IP_3Rs regulate hypertensive blood pressure. Hypertension was induced by chronic AngII infusion, and blood pressure was measured using the tail cuff system. First, we confirmed that basal systolic blood pressure in smTKO mice was not significantly different from that in control mice (121.3 ± 1.6 mmHg in smTKO mice vs. 118.1 ± 2.4 mmHg in control mice; Figure 5A), consistent with the data from the telemetry analysis. By contrast, deletion of IP_3Rs reduced AngII-induced hypertension. Systolic blood pressure was measured before AngII infusion and every 7 days after AngII infusion. Systolic blood pressures of control mice gradually increased and reached peak levels within 2 weeks after AngII

infusion (Figure 5B). Deletion of IP_3Rs in VSMCs significantly diminished the elevation of systolic blood pressure at all time points (1 week, 137.3 ± 3.0 mmHg in control vs. 126.6 ± 1.9 mmHg in smTKO; 2 weeks, 147.2 ± 4.1 mmHg in control vs. 134.4 ± 2.1 mmHg in smTKO; 3 weeks, 139.0 ± 4.4 mmHg in control vs. 126.3 ± 2.5 mmHg in smTKO; Figure 5B).

Finally, we analyzed the structure of the thoracic aorta by histology to determine if IP_3R deletion influenced vascular remodeling induced by AngII. The medial thickness of the thoracic aorta was measured before and after AngII infusion. No significant changes in medial thickness of the thoracic aorta were observed in smTKO and control mice before and after AngII infusion (33.5 ± 1.7 μm in control mice vs. 34.5 ± 1.8 μm in smTKO mice before AngII infusion; 53.4 ± 3.9 μm in control mice vs. 55.4 ± 3.5 μm in smTKO mice 4 weeks after AngII infusion; Figure 5, C and D), suggesting that deletion of IP_3Rs has no apparent effect on AngII-induced vascular remodeling.

Discussion

Signaling systems that are downstream of cytoplasmic free Ca^{2+} concentration modulation are involved in the regulation of numerous processes, including muscle contraction, synaptic transmission, membrane excitation, secretion, learning and memory, gene expression, cell differentiation, and apoptosis. A ubiquitous mechanism for Ca^{2+} signaling is release from intracellular compartments. GPCRs activating PLCβ, and tyrosine kinase receptors activating PLCγ, cleave phosphatidylinositol 4, 5-bisphosphate into IP_3 and diacylglycerol. IP_3 binding to IP_3Rs, intracellular ligand-gated Ca^{2+} release channels localized primarily in the ER membrane, allows diffusion of Ca^{2+} from the ER to increase intracellular $[Ca^{2+}]_i$. It has been established that 3 different genes encode for a family of IP_3Rs in mammalian cells, including humans and other vertebrates (28). In mammals, IP_3Rs are ubiquitously expressed, perhaps in all cell types, and the 3 subtypes have distinct and overlapping patterns of expression, with most cells outside the central nervous system expressing more than one type. In cultured VSMCs, our results demonstrated that all 3 IP_3R channels were present at mRNA and protein levels. In addition, all 3 IP_3Rs were observed in intact aortas. More importantly, the mRNA and protein levels of all 3 IP_3Rs were dramatically reduced after tamoxifen-induced gene deletion in adult smooth muscle cells, demonstrating that all 3 IP_3R channels are substantially expressed in VSMCs, which is consistent with several prior studies (20–22). The overlapping expression of IP_3Rs in VSMCs may suggest functional redundancy between subtypes. Indeed, evidence from both in vitro and in vivo studies has suggested that there is functional redundancy among the IP_3R subtypes. For example, deletion of IP_3R2/IP_3R3 together was required to generate a pancreatic acinar cell secretion phenotype (9), genetic IP_3R1 single deletion or any combination of IP_3R double deletion was without effect on T cell development (15, 29), deletion of all 3 IP_3Rs resulted in T cell developmental defects and T cell leukemia (15), and genetic deletion of IP_3R1/IP_3R2 or IP_3R1/IP_3R3 was required to cause an early embryonic lethality (13, 14). In this study, we investigated if IP_3Rs exhibit functional redundancy in modulating intracellular Ca^{2+} signals in VSMCs. We found that single deletion of IP_3R1 in cultured VSMCs only reduced ATP-induced Ca^{2+} signals by approximately 50%, whereas triple deletion of all IP_3Rs decreased ATP-induced Ca^{2+} signals by more than 90%, suggesting that IP_3R2 and IP_3R3 are functional in regulating Ca^{2+} release from the ER in response to GPCR activation, which is also partially consistent with a previous study using IP_3R1 knockout and IP_3R2/IP_3R3 double-knockout cells (22).

VSMCs are a type of specialized smooth muscle cells, which reside within the medial layer of blood vessels. The primary function of VSMCs is to control blood vessel diameter in response to intraluminal pressure and various physiologic stimuli emanating from the central nervous system, kidneys, and local tissues. Elevation of intracellular Ca^{2+} is a key step required for increasing the contractile activity of VSMCs. Elevated Ca^{2+} results in increased levels of Ca^{2+}-calmodulin (Ca^{2+}/CaM), which has a high affinity for the inactive MLCK (26). The binding of Ca^{2+}/CaM to MLCK leads to phosphorylation of MLC20 at Ser19, enabling molecular crossbridge formation between myosin and actin filaments. The essential role of Ca^{2+} entry via VOCCs has been well established, since VOCC blockers have been widely used to reduce high blood pressure in hypertensive patients (1, 2). However, the role of IP_3Rs in regulating vascular contractility and blood pressure is not well understood because (a) genetic deletion of IP_3R1 or double deletion of any two IP_3R subtypes causes developmental defects and invariably leads to premature lethality (8, 9, 13, 14) and (b) there has been a lack of a smooth muscle–specific IP_3R knockout mouse model. Here, we generated a mouse model in which all 3 IP_3R subtypes were specifically deleted in adult mouse smooth muscle cells in a tamoxifen-inducible manner, which allowed us to overcome the premature lethality and the secondary

vascular defects resulting from global IP_3R gene deletion. Furthermore, since all 3 IP_3R subtypes could be simultaneously deleted, our mouse model provides a powerful tool for investigating the physiological and pathological roles of smooth muscle IP_3R-mediated Ca^{2+} signaling in vivo, with no necessity of considering the functional redundancy between IP_3R subtypes.

In VSMCs, vasoconstrictor pathways may be coupled directly to intracellular activation of Gq/11- and G12/13-mediated intracellular signaling, in which IP_3R-mediated Ca^{2+} release is downstream of Gq/11 activation. In parallel, activation of Gq/11 and G12/13 could also induce vasoconstrictive responses via PKC and Rho/Rho kinase. It has been shown that Gq/11-mediated signaling pathways are required for maintenance of basal blood pressure and for the development of salt-induced hypertension. Deletion of Gq/11 in adult mouse VSMCs results in abolished vasoconstrictive responses, lower basal blood pressure, and reduced salt-induced hypertension (25). Importantly, we found that force generation of IP_3R-deficient aortas was reduced in response to multiple vasoconstrictors, such as PE, U46619, 5-HT, and ET1, suggesting that IP_3R-mediated Ca^{2+} release plays an important role in regulating vascular contraction following activation of GPCR, which is consistent with previous studies using the IP_3R blockers heparin, 2-APB, or Xestospongin (30–33). Our results also suggested that both IP_3R-dependent and IP_3R-independent pathways could contribute to Gq/11-mediated regulation of vascular contraction, since deletion of Gq/11 has much more efficacy in reducing vasoconstrictive responses than deletion of IP_3Rs. Furthermore, we also showed that diminished force production is consistent with decreased levels of MLC20 phosphorylation at Ser19 and MYPT1 phosphorylation at Thr853, whereas deletion of IP_3Rs does not affect the basal expression of MLC20 and MYPT1. However, we did not identify altered expression of major Ca^{2+} regulatory proteins, such as *Ryr2*, *Ryr3*, *Cav1.2*, *Stim1*, and *Stim2*, in IP_3R-deficient aortas. The expression of major vasoconstrictor receptors, excluding that of *Ednra*, was also comparable between control and IP_3R-deficient vessels. Together, these results suggest that inducible deletion of IP_3Rs in adult VSMCs diminishes vasoconstrictive responses, while major components of Ca^{2+} signaling networks are maintained.

Tamoxifen-induced deletion of IP_3Rs in adult mouse VSMCs did not affect basal blood pressure measured by the telemetry system as well as the tail-cuff method. In addition, application of 2-APB to block residual IP_3Rs in smTKO vessels did not cause a further decrease in AngII-induced contraction. Together, these data indicated that IP_3R-mediated Ca^{2+} release might not be required for the maintenance of physiological blood pressure. The absence of any modification of basal blood pressure in IP_3R-deficient mice correlates well with the nonalteration of their vascular histology. By contrast, inducible deletion of Gq/11 in adult mouse VSMCs resulted in a sustained decrease of basal blood pressure (25). This difference between the two mouse models suggests that IP_3R-independent mechanisms, following Gq/11 activation, but not IP_3R-dependent mechanisms, play a major role in controlling basal blood pressure. We also hypothesize that the difference might directly come from the varied vasoconstrictive responses to adrenergic stimulation in these two mouse models. Loss of IP_3Rs in VSMCs only partially reduced, but deletion of Gq/11 in VSMCs totally abrogated, PE-induced vascular contraction. Similarly, a significant decrease in PE-induced vasoconstrictive response was found in both Wnk1 heterozygous mice and α1b-adrenergic receptor knockout mice, but both mice developed normal basal blood pressure (34–36). Interestingly, we found that IP_3R-mediated Ca^{2+} signaling plays an important role in AngII-induced hypertension. Loss of IP_3Rs in VSMCs significantly attenuated the elevation of blood pressure in a hypertensive state induced by chronic AngII infusion. It has been proposed that increased RhoA and Rock activities play a causative role in the pathogenesis of AngII-induced hypertension (27). We showed that loss of IP_3Rs in VSMCs caused blunted MYPT1 phosphorylation in response to acute vasoconstrictive stimulation. However, it remains to be determined if deficiency of IP_3Rs could lead to a sustained repression of MYPT1 activation upon chronic AngII stimulation. Furthermore, arterial wall thickness in IP_3R-deficient mice was comparable to that of control mice, suggesting that neither elevated blood pressure nor IP_3R-mediated Ca^{2+} signaling is required for AngII-induced vascular remodeling.

In summary, we provided a mouse model with the deletion of all 3 IP_3R subtypes in adult smooth muscle cells and demonstrated that IP_3R-mediated Ca^{2+} release plays an important role in regulating vascular contractility and AngII-induced hypertension.

Methods

Mice. The generation of floxed alleles of the genes encoding IP_3R1, IP_3R2, and IP_3R3 has been described previously (15, 37). We used two different tissue-specific Cre recombinases to delete IP_3Rs in VSMCs. First, we crossed IP_3R1 flox ($IP_3R1^{f/f}$) mice or IP_3R triple flox ($IP_3R1^{f/f}IP_3R2^{f/f}IP_3R3^{f/f}$) mice with Tg(Ta-

gln-cre)1Her/J (Sm22α-Cre) mice (The Jackson Laboratory), respectively. IP_3R triple flox mice had been backcrossed with C57BL/6 mice for more than 7 generations. Sm22α-Cre is constitutively expressed and has been frequently used as a smooth muscle–specific Cre (38). Second, mice with inducible deletion of all 3 IP_3R genes were generated by crossing IP_3R triple flox mice with B6.FVB-Tg(Myh11-Cre/ERT2)1Soff/J (SMMHC-CreER^{T2}) mice (The Jackson Laboratory). Since the SMMHC-Cre gene is located on the Y chromosome in this mouse line, only male offspring carried the SMMHC-Cre gene (25). Thus, in our study, we characterized only male mice. Male $IP_3R1^{f/f}IP_3R2^{f/f}$ $IP_3R3^{f/f}$/SMMHC-Cre$^+$ mice aged 7 to 8 weeks were intraperitoneally injected with tamoxifen (50 mg/kg/d) for 5 consecutive days to delete IP_3R genes and were considered as considered as smTKO mice. Male $IP_3R1^{f/f}IP_3R2^{f/f}$ $IP_3R3^{f/f}$/SMMHC-Cre$^-$ mice treated with tamoxifen and male noninduced smTKO mice were used as control mice. All mice were housed under a 12-hour-day/night cycle at a temperature of 25°C.

Cell culture and calcium imaging. Thoracic aortas were isolated from young male noninduced smTKO mice and cut into small pieces. The tissue explants were then spread over gelatin-coated (1%) dishes and cultured in DMEM supplemented with 20% FBS at 37°C. After passage 1, VSMCs were cultured in DMEM supplemented with 10% FBS and used between passages 3 and 6. Deletion of IP_3R genes was induced by adding 4OHT (1 μM, Sigma-Aldrich) into the medium. Both the efficiency of gene deletion and calcium imaging were performed 72 hours after induction.

For Ca^{2+} imaging in cultured VSMCs, cells were washed twice with physiological saline solution ([PSS] in mM: NaCl 137, KCl 5.4, $MgSO_4$ 1.0, glucose 10, $CaCl_2$ 1.8, and HEPES 10, pH 7.4), followed by incubation with fluo-4-AM (5 μM, 30 minutes, 37°C; F14201, Invitrogen). Cells were imaged with a Zeiss LSM510 inverted confocal microscope. In order to avoid the potential Ca^{2+} entry via membrane ionotropic purinergic receptors, cells were perfused with a Ca^{2+}-free PSS (0 [Ca^{2+}] plus 1.0 mM EGTA) for a short time (1–2 minutes) before the administration of ATP (10 μM, Sigma-Aldrich). On the other hand, the cells were incubated in regular PSS when 5-HT (10 μM; Sigma-Aldrich), U46619 (0.1 μM; Sigma-Aldrich), and ET1 (1.0 μM; Sigma-Aldrich) were applied to induce intracellular Ca^{2+} mobilization. At least 20 cells per dish were imaged. Image processing and data analysis were performed as previously described (39).

For Ca^{2+} imaging in intact vessels, segments of posterior cerebral artery were isolated from control and smTKO mice and cannulated, as previously described (40), and incubated in the dark with fluo-4-AM (10 μM) and 0.05% Pluronic F-127 (Invitrogen) for 1 hour, followed by a 20-minute wash. Intracellular Ca^{2+} signals in cerebral artery smooth muscle cells were imaged using a Zeiss 5-live confocal system. The fluorescence was excited with 488-nm light, and emitted light >510 nm was collected. Images (512 × 254 pixels) were acquired at a rate of 30 per second. At least two different representative areas were scanned for 40 seconds in each arterial segment. Only those propagating Ca^{2+} events with $F/F0 > 1.2$ were counted as Ca^{2+} waves. Ca^{2+} wave frequency was analyzed offline using ImageJ 1.49 (NIH).

Quantitative reverse transcription–PCR. Total RNA was extracted from thoracic aortas or cultured VSMCs using Trizol reagent (Invitrogen), and cDNA was synthesized using the *TransScript* One-Step cDNA Synthesis SuperMix Kit (Transgen Biotech). Quantitative real-time PCR was performed using *TransStart* Tip Green qPCR SuperMix (Transgen Biotech) according to the manufacturer's instructions. Sequences of primers used for PCR can be found in Supplemental Table 1. Values are expressed as the $2^{-\Delta Ct}$ value relative to *Gapdh* in each sample. All quantitative real-time PCR experiments were performed in triplicate on each sample.

Western blotting. Protein lysates were prepared from smooth muscle layers of thoracic aortas or cultured VSMCs using a protein lysis buffer containing 8 M urea, 2 M thiourea, 3% SDS, 75 mM DTT, 0.05 M Tris-HCl (pH 6.8), and 0.03% bromophenol blue. After performing ultrasonication 3 times (for 3 seconds each time), lysates were centrifuged for 5 minutes at 15,294 rpm at 4°C. The supernatants were then heated at 95°C for 5 minutes. To examine IP_3R protein expression, proteins were separated by 6% SDS-PAGE gel and transferred to a 0.45-μm PVDF membrane (Millipore). The primary antibodies against mouse IP_3R1 and IP_3R2 were raised in our lab as previously described (15). The antibodies against mouse IP_3R3 (BD Bioscience, catalog 610312), MLCK (Abcam, catalog ab76092), SMA (Invitrogen, catalog 180106), SM22α (Abcam, catalog ab14106), and β-actin (Santa Cruz Biotechnology, catalog sc-47778) were commercially purchased.

To examine the phosphorylation levels of the contractile proteins, thoracic aortas were teased from connective tissues and incubated with indomethacin (10 μM, Sigma-Aldrich) and nitro-L-arginine (100 μM, Sigma-Aldrich) to inhibit endothelial function at 37°C for 30 minutes. The vehicle (PSS) and U46619 (0.1 μM) were then added, and the tissues were incubated for another 20 minutes. After that, the tissues were snap frozen in liquid nitrogen, and homogenized using the lysis buffer as described above. The pri-

mary antibodies against MLC20, phosphorylated MLC20 at Ser19, myosin phosphatase target subunit 1 (MYPT1), and phosphorylated MYPT1 at Thr853 were purchased from Cell Signaling Technology (catalog 8505, catalog 3671, catalog 2634P, and catalog 14563P, respectively).

Myography. For isometric tension recordings, thoracic aortas and the first-order branch of superior mesenteric arteries were isolated from mice and rinsed in ice-cold Krebs solution (in mM: NaCl 118, KCl 4.6, $NaHCO_3$ 25, $CaCl_2$ 2.5, $MgSO_4$ 1.2, KH_2PO_4 1.2, glucose 12, pH 7.4). After removing the connective tissues, the vessels were cut into 2-mm-long segments and mounted in a myograph chamber (620 M, Danish Myo Technology) filled with 5 ml Krebs solution aerated with 95% O_2–5% CO_2 and maintained at 37°C. Each vessel ring was stretched in a stepwise fashion to the optimal resting tension (thoracic aortas to ~9 mN; mesenteric arteries to ~1.5 mN), equilibrated for 30 minutes, and exposed to 100 mM K^+ Krebs solution to elicit a reference contraction. An inhibitor of cyclooxygenases, indomethacin (10 μM, Sigma-Aldrich), and an inhibitor of endothelial nitric oxide synthase, nitro-L-arginine (100 μM, Sigma-Aldrich), was added and incubated for at least 30 minutes prior to agonist dose-response curves. Thereafter, PE (a α-adrenergic receptor agonist; 1 nM to 10 μM), U46619 (a thromboxane A2 receptor agonist; 1 nM to 0.1 μM), 5-HT (a serotonin receptor agonist; 1 nM to 10 μM), ET1 (an endothelin receptor agonist; 0.1 nM to 0.1 μM), and AngII (an angiotensin receptor agonist; 0.01 nM to 0.1 μM; Sigma-Aldrich) were applied individually to distinct vessels to stimulate contraction. IP_3R antagonist 2-APB (50 μM, Sigma-Aldrich) was used to treat the vessels for 30 minutes prior to the application of AngII. The contractile responses to the cumulatively administrated vasoconstrictive agonists were recorded in the presence of indomethacin and nitro-L-arginine. Data were expressed as increases in force and as percentages of the peak of K^+-induced contraction.

Measurement of blood pressure using a tail-cuff system. Blood pressure was measured using a noninvasive computerized tail-cuff system (NIBP system, IN125/m, AD Instruments). After the mice were placed in a plastic holder, the occlusion and sensor cuff were positioned on the base of the tail. All the mice were given at least 1 week to adapt to the system prior to blood pressure measurement. Blood pressure was measured at least 6 times in each mouse.

To produce hypertensive mice, AngII was infused chronically at a rate of 490 ng/kg/min for 21 consecutive days via a subcutaneously implanted osmotic mini-pump (Alzet 2004). The blood pressure of each mouse was measured at day –1, day 7, day 14, and day 21 after implantation.

Telemetry measurements. Blood pressure and heart rate were measured in conscious, unrestrained mice using a radiotelemetry system (PA-C10 and Dataquest software, Data Sciences International). After a week recovery period from surgery, recordings were obtained every 15 minutes for 60 seconds and each mouse was monitored for 3 consecutive days. The data were analyzed for two 12-hour periods (from 8:00 to 20:00 for daytime and from 20:00 to 8:00 for nighttime) to evaluate circadian variation in hemodynamics.

Histology. Thoracic aortas were harvested and fixed in 4% paraformaldehyde at 4°C overnight. Tissues were embedded in paraffin, and 8-μm sections were taken and mounted on glass slides. Sections were stained by H&E and examined by light microscopy. Aortic medial thickness was measured from the internal elastic lamina to the adventitial border. Analysis was performed using at least 3 different sections from each mouse and quantified with ImageJ (NIH) software.

Statistics. Box-and-whisker plots were presented using GraphPad Prism 5. *P* values were calculated using a 2-tailed, unpaired Student's *t* test or 2-way ANOVA with Bonferroni post-hoc test for multiple comparisons. Data represent mean ± SEM. $P < 0.05$ was considered statistically significant.

Study approval. All animal care and use procedures in this study were approved by the Animal Care and Use Committee at UCSD (San Diego, USA) and at Peking University Shenzhen Graduate School (Shenzhen, China), respectively. Periodic review of procedures was performed, and amendments were made as needed.

Author contributions

QL, GZ, XP, HT, HW, and RJ performed research; KO, XF, JL, WJL, and JC designed the research; and KO, XF, GZ, WJL, and JC wrote the manuscript.

Acknowledgments

The authors would like to thank Yu Huang (The Chinese University of Hong Kong) for critical suggestions about experimental design and Jennifer Veevers for critical reading of the manuscript. The work was supported by the National Key Basic Research Program of China (2013CB531200), the Shenzhen Basic Research Foundation (JCYJ20140509093817680 and JCYJ20160428154108239), the National Science

Foundation of China (31370823, 91439130), and the National Institutes of Health (JC). JC is the American Heart Association Endowed Chair in Cardiovascular Research. GZ is also supported by a National Scientist Development Grant (10SDG4030042) from the American Heart Association. RJ was also supported by the Hunan Province's Science and Technology Project (2015SK2026).

Address correspondence to: Ju Chen, Department of Medicine, University of California San Diego, 9500 Gilman Drive, La Jolla, California, 92093-0613C, USA. Phone: 858.822.4276; E-mail: juchen@ucsd.edu. Or to: Kunfu Ouyang, Drug Discovery Center, Key Laboratory of Chemical Genomics, Peking University Shenzhen Graduate School, Shenzhen, China. Phone: 86.755.26506501; E-mail: ouyangkunfu@pkusz.edu.cn.

1. Conlin PR, Williams GH. Use of calcium channel blockers in hypertension. *Adv Intern Med*. 1998;43:533–562.
2. Cummings DM, Amadio P, Nelson L, Fitzgerald JM. The role of calcium channel blockers in the treatment of essential hypertension. *Arch Intern Med*. 1991;151(2):250–259.
3. Haller H. Effective management of hypertension with dihydropyridine calcium channel blocker-based combination therapy in patients at high cardiovascular risk. *Int J Clin Pract*. 2008;62(5):781–790.
4. De Smedt H, et al. Determination of relative amounts of inositol trisphosphate receptor mRNA isoforms by ratio polymerase chain reaction. *J Biol Chem*. 1994;269(34):21691–21698.
5. Grayson TH, Haddock RE, Murray TP, Wojcikiewicz RJ, Hill CE. Inositol 1,4,5-trisphosphate receptor subtypes are differentially distributed between smooth muscle and endothelial layers of rat arteries. *Cell Calcium*. 2004;36(6):447–458.
6. Islam MO, Yoshida Y, Koga T, Kojima M, Kangawa K, Imai S. Isolation and characterization of vascular smooth muscle inositol 1,4,5-trisphosphate receptor. *Biochem J*. 1996;316(Pt 1):295–302.
7. Morel JL, Fritz N, Lavie JL, Mironneau J. Crucial role of type 2 inositol 1,4,5-trisphosphate receptors for acetylcholine-induced Ca2+ oscillations in vascular myocytes. *Arterioscler Thromb Vasc Biol*. 2003;23(9):1567–1575.
8. Matsumoto M, et al. Ataxia and epileptic seizures in mice lacking type 1 inositol 1,4,5-trisphosphate receptor. *Nature*. 1996;379(6561):168–171.
9. Futatsugi A, et al. IP3 receptor types 2 and 3 mediate exocrine secretion underlying energy metabolism. *Science*. 2005;309(5744):2232–2234.
10. Inaba T, et al. Mice lacking inositol 1,4,5-trisphosphate receptors exhibit dry eye. *PLoS One*. 2014;9(6):e99205.
11. Orabi AI, et al. IP3 receptor type 2 deficiency is associated with a secretory defect in the pancreatic acinar cell and an accumulation of zymogen granules. *PLoS One*. 2012;7(11):e48465.
12. Hisatsune C, et al. Abnormal taste perception in mice lacking the type 3 inositol 1,4,5-trisphosphate receptor. *J Biol Chem*. 2007;282(51):37225–37231.
13. Nakazawa M, et al. Inositol 1,4,5-trisphosphate receptors are essential for the development of the second heart field. *J Mol Cell Cardiol*. 2011;51(1):58–66.
14. Uchida K, et al. Gene knock-outs of inositol 1,4,5-trisphosphate receptors types 1 and 2 result in perturbation of cardiogenesis. *PLoS One*. 2010;5(9):e12500.
15. Ouyang K, et al. Loss of IP3R-dependent Ca2+ signalling in thymocytes leads to aberrant development and acute lymphoblastic leukemia. *Nat Commun*. 2014;5:4814.
16. Bastin G, Heximer SP. Intracellular regulation of heterotrimeric G-protein signaling modulates vascular smooth muscle cell contraction. *Arch Biochem Biophys*. 2011;510(2):182–189.
17. Sanders KM. Invited review: mechanisms of calcium handling in smooth muscles. *J Appl Physiol*. 2001;91(3):1438–1449.
18. Koida S, Ohyanagi M, Ueda A, Mori Y, Iwasaka T. Mechanism of increased alpha-adrenoceptor-mediated contraction in small resistance arteries of rats with heart failure. *Clin Exp Pharmacol Physiol*. 2006;33(1-2):47–52.
19. Lee CH, et al. Sequential opening of IP(3)-sensitive Ca(2+) channels and SOC during alpha-adrenergic activation of rabbit vena cava. *Am J Physiol Heart Circ Physiol*. 2002;282(5):H1768–H1777.
20. Tykocki NR, Wu B, Jackson WF, Watts SW. Divergent signaling mechanisms for venous versus arterial contraction as revealed by endothelin-1. *J Vasc Surg*. 2015;62(3):721–733.
21. Tasker PN, Taylor CW, Nixon GF. Expression and distribution of InsP(3) receptor subtypes in proliferating vascular smooth muscle cells. *Biochem Biophys Res Commun*. 2000;273(3):907–912.
22. Zhou H, et al. Predominant role of type 1 IP3 receptor in aortic vascular muscle contraction. *Biochem Biophys Res Commun*. 2008;369(1):213–219.
23. Zhao G, et al. Type 1 IP3 receptors activate BKCa channels via local molecular coupling in arterial smooth muscle cells. *J Gen Physiol*. 2010;136(3):283–291.
24. Shen Z, et al. Smooth muscle protein 22 alpha-Cre is expressed in myeloid cells in mice. *Biochem Biophys Res Commun*. 2012;422(4):639–642.
25. Wirth A, et al. G12-G13-LARG-mediated signaling in vascular smooth muscle is required for salt-induced hypertension. *Nat Med*. 2008;14(1):64–68.
26. Ogut O, Brozovich FV. Regulation of force in vascular smooth muscle. *J Mol Cell Cardiol*. 2003;35(4):347–355.
27. Loirand G, Pacaud P. Involvement of Rho GTPases and their regulators in the pathogenesis of hypertension. *Small GTPases*. 2014;5(4):1–10.
28. Foskett JK, White C, Cheung KH, Mak DO. Inositol trisphosphate receptor Ca2+ release channels. *Physiol Rev*. 2007;87(2):593–658.
29. Hirota J, Baba M, Matsumoto M, Furuichi T, Takatsu K, Mikoshiba K. T-cell-receptor signalling in inositol 1,4,5-trisphosphate

receptor (IP3R) type-1-deficient mice: is IP3R type 1 essential for T-cell-receptor signalling? *Biochem J*. 1998;333(Pt 3):615–619.
30. Hashimoto T, et al. Heparin recovers AT1 receptor and its intracellular signal transduction in cultured vascular smooth muscle cells. *FEBS Lett*. 2005;579(1):281–284.
31. Kobayashi S, Kitazawa T, Somlyo AV, Somlyo AP. Cytosolic heparin inhibits muscarinic and alpha-adrenergic Ca2+ release in smooth muscle. Physiological role of inositol 1,4,5-trisphosphate in pharmacomechanical coupling. *J Biol Chem*. 1989;264(30):17997–18004.
32. Lamont C, Wier WG. Different roles of ryanodine receptors and inositol (1,4,5)-trisphosphate receptors in adrenergically stimulated contractions of small arteries. *Am J Physiol Heart Circ Physiol*. 2004;287(2):H617–H625.
33. Maejima D, Kawai Y, Ajima K, Ohhashi T. Platelet-derived growth factor (PDGF)-BB produces NO-mediated relaxation and PDGF receptor β-dependent tonic contraction in murine iliac lymph vessels. *Microcirculation*. 2011;18(6):474–486.
34. Bergaya S, et al. WNK1 regulates vasoconstriction and blood pressure response to α 1-adrenergic stimulation in mice. *Hypertension*. 2011;58(3):439–445.
35. Cavalli A, et al. Decreased blood pressure response in mice deficient of the alpha1b-adrenergic receptor. *Proc Natl Acad Sci U S A*. 1997;94(21):11589–11594.
36. Vecchione C, et al. Cardiovascular influences of alpha1b-adrenergic receptor defect in mice. *Circulation*. 2002;105(14):1700–1707.
37. Li X, Zima AV, Sheikh F, Blatter LA, Chen J. Endothelin-1-induced arrhythmogenic Ca2+ signaling is abolished in atrial myocytes of inositol-1,4,5-trisphosphate(IP3)-receptor type 2-deficient mice. *Circ Res*. 2005;96(12):1274–1281.
38. Holtwick R, et al. Smooth muscle-selective deletion of guanylyl cyclase-A prevents the acute but not chronic effects of ANP on blood pressure. *Proc Natl Acad Sci U S A*. 2002;99(10):7142–7147.
39. Ouyang K, Wu C, Cheng H. Ca(2+)-induced Ca(2+) release in sensory neurons: low gain amplification confers intrinsic stability. *J Biol Chem*. 2005;280(16):15898–15902.
40. Zhao G, Adebiyi A, Blaskova E, Xi Q, Jaggar JH. Type 1 inositol 1,4,5-trisphosphate receptors mediate UTP-induced cation currents, Ca2+ signals, and vasoconstriction in cerebral arteries. *Am J Physiol, Cell Physiol*. 2008;295(5):C1376–C1384.